

Supporting Information:

Excitation Wavelength Dependent O₂ Release from Copper(II)-Superoxide Compounds: Laser Flash-Photolysis Experiments and Theoretical Studies

Claudio Saracini[†], Dimitrios G. Liakos[‡], Jhon E. Zapata Rivera[§], Frank Neese[‡], Gerald J. Meyer[†], and Kenneth D. Karlin^{*†}

[†]*Department of Chemistry, The Johns Hopkins University, Baltimore, Maryland 21218*

[‡]*Max-Planck-Institut für Chemische Energie Konversion, Stiftstrasse 34-36, 45470 Mülheim*

[§]*Departament de Química Física i Inorgànica, Universitat Rovirai Virgili, c/ Marcel·lí Domingo, s/n. 43007 Tarragona, Spain*

*To whom correspondence should be addressed: EMAIL: karlin@jhu.edu

Contents:

1. **Materials and Methods**
2. **Determination of O₂ solubility in 2-MeTHF**
3. **Gas Mixing**
4. **Transient Absorption Experimental Details**
5. **Data Treatment for Benchtop Titration Measurements**
6. **Model Used for the Kinetic Studies**
7. **Quantum Efficiency Measurements**
8. **DFT Calculations**
9. **Table S(1): Comparison of Equilibrium Parameters Determined with Two Different Methods**
10. **Figure S(1): Fit for the Determination of the Equilibrium Constant at -65⁰C**
11. **Figure S(2): Van't Hoff Plot Determined from Benchtop Titration Experiments**
12. **Figure S(3): Determination of k_{O_2} and k_{-O_2} in Pseudo-First-Order Conditions**
13. **Figure S(4): Eyring Analysis on Data Obtained from Transient Absorption Spectroscopy Exciting with either $\lambda_{exc} = 436$ nm or $\lambda_{exc} = 683$ nm Light**
14. **Figure S(5): Van't Hoff Plot Determined from Transient Absorption Spectroscopic Data**
15. **Figure S(6): Molecular Orbital Diagram for the [(TMG₃tren)Cu(O₂)]⁺ Ground State**
16. **Figure S(7): Calculated O-O Bond Length Trend upon Cu-O Bond Stretching**
17. **Figure S(8): Relation Between K_{O_2} and Solvent Dielectric Constant**
18. **Figure S(9): Transient Absorption Spectra Obtained for 1 using $\lambda_{exc} = 436$ and 683 nm light**
19. **Figure S(10): Absorption Spectra and Transient Absorption Spectra of 2 and 4**
20. **Figure S(11): Estimation of Activation Parameters for 4 + O₂ -> 2: Eyring plot**
21. **References**

1. Materials and Methods

All materials purchased were of highest purity available from Sigma-Aldrich Chemical or Tokyo Chemical Industries (TCI) and used as received, unless specified otherwise. 2-Methyltetrahydrofuran (MeTHF) and tetrahydrofuran were distilled under an inert atmosphere from Na/benzophenone and degassed with argon prior to use. Pentane and acetonitrile were freshly distilled from calcium hydride under an inert atmosphere and degassed prior to use. $[(\text{TMG}_3\text{tren})\text{Cu}^{\text{I}}]\text{BArF}$ and $[\text{Cu}^{\text{I}}(\text{MeCN})_4]\text{BArF}$ were synthesized according to literature protocols,¹ and their identity and purity were verified by elemental analysis and/or $^1\text{H-NMR}$. Synthesis and manipulations of copper salts were performed according to standard Schlenk techniques or in an MBraun glovebox (with O_2 and H_2O levels below 1 ppm). UV-Vis spectra were recorded with a Cary 50 Bio spectrophotometer equipped with a liquid nitrogen chilled Unisoku USP-203-A cryostat. NMR spectroscopy was performed on Bruker 300 and 400 MHz instruments with spectra calibrated to either internal tetramethylsilane (TMS) standard or to residual protio solvent. The ligands (TMG₃tren and PV-TMPA) and the related copper(I) complexes ($[(\text{TMG}_3\text{tren})\text{CuI}]\text{BArF}$ and $[(\text{PV-TMPA})\text{CuI}]\text{BArF}$) were synthesized by literature procedures.^{1a, 2}

2. Determination of O₂ solubility in 2-MeTHF

The solubility of O_2 in 2-MeTHF was determined using mole fractions and temperature-dependent data given in the literature.³ The molar fraction solubility of $\text{O}_{2(\text{g})}$ in 2-MeTHF at 1 atmosphere and 311.03 K was extrapolated from the available data to be $5.79973 \cdot 10^{-4}$. Molar fraction solubility at different temperatures were obtained using the data available for the molar fraction solubility of $\text{O}_{2(\text{g})}$ in diethyl ether as a function of temperature⁴ fitting the data to the experimentally determined from Ref. 3.

3. Gas Mixing

Carbon monoxide (CO ; Air Gas East, grade 2.3) used for the flash-and-trap experiment performed for $[(\text{TMPA})\text{Cu}^{\text{I}}(\text{CO})]\text{BArF}$ in 2-MeTHF was treated by passing through an R & D Separations oxygen/moisture trap (Agilent Technologies OT3-4). Dioxygen (O_2 ; Air Gas East, grade 4.4) was dried by passing the gas through a short column of supported P4010 (Aquasorb, Mallinkrodt). Red rubber tubing (Fisher Scientific; inner diameter: 1/4 in.; thickness: 3/16 in.) was used to attach the gas cylinders fitted with appropriate regulators to two MKS Instruments Mass-Flo Controllers (MKS Type 1179A) regulated by an MKS Instruments Multi-Channel Flow Ratio/Pressure Controller (MKS Type 647C). The gas mixtures (N_2/CO and O_2/CO for $[(\text{TMPA})\text{Cu}^{\text{I}}(\text{CO})]\text{BArF}$ and N_2/O_2 for $[(\text{TMG}_3\text{tren})\text{Cu}(\text{O}_2)]\text{BArF}$ and $[(\text{PV-TMPA})\text{Cu}(\text{O}_2)]\text{BArF}$) were determined by the set flow rates of the two gases. For example, a 10% O_2 mixture would be made by mixing O_2 at a rate of 10 standard cubic centimeters per minute (sccm) with CO at 90 sccm for a total flow of 100 sccm. By varying the ratio of O_2 and CO with the gas mixer, the concentration of the gases were determined by taking the percentage of the gas added and multiplying by the solubility of the corresponding gas in 2-MeTHF. For example, if $[\text{O}_2] = 0.0087 \text{ M}$ and $[\text{CO}] = 0.0092 \text{ M}$ at -70°C , if the O_2/CO flow rate is 3/7 (or

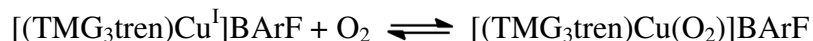
30% of the total gas flow is O₂), then, the concentration of O₂ in 2-MeTHF = 0.30 x 0.0087 M = 0.0026 M and CO = 0.70 x 0.0092 M = 0.0064 M.

4. Transient Absorption Experimental Details

Experimental information for the setup of the Nd:YAG flash-photolysis apparatus has been previously reported.⁵ The apparatus was equipped with liquid nitrogen chilled Unisoku USP-203-A cryostat and a pressurized (~400 psi) H₂ Raman shifter tube to obtain the Stokes-shifted 683 and the anti-Stokes-shifted 436 nm excitation wavelengths. The samples, [(TMG₃tren)Cu(O₂)]BArF and [(PV-TMPA)Cu(O₂)]BArF, were irradiated with λ_{ex} = 436 nm or λ_{ex} = 683 nm pulsed light (15 mJ/pulse) and data was collected at the monitored wavelengths from averages of 60 laser pulses. Samples (320-360 μM) were prepared under an inert atmosphere (drybox) in 1 cm quartz cuvettes with four polished windows made custom by Quark glass. The cuvettes were equipped with a 14/20 joint and Schlenk stopcock. Gas mixtures were added to sample solutions through direct bubbling through a 24-inch needle (19-gauge) for 5 seconds for 10 times with intervals of 10 seconds between each time. During data collection the gas flowed through the headspace of the sample solution into the cuvette.

5. Data Treatment for Benchtop Titration Measurements

The equilibrium constant for the following chemical reaction



can be written as

$$K_{\text{O}_2} = [\text{LCuO}_2] / [\text{LCu}^{\text{I}}] [\text{O}_2] \quad (1)$$

having called TMG₃tren = L and having omitted the counter anion BArF for simplicity. Substitution of [LCu^I] = [LCu^I]₀ - [LCuO₂] (2) into (1) (where [LCu^I]₀ is the initial concentration of LCu^I, before adding O₂), gives equation (3):

$$[\text{LCuO}_2] / [\text{O}_2] = K_{\text{O}_2} ([\text{LCu}^{\text{I}}]_0 - [\text{LCuO}_2]) \quad (3)$$

Considering, now, that O₂ does not absorb light at the wavelength λ = 449 nm, we choose to monitor LCu^I and LCuO₂. Consequently, the total observed absorbance at 449 nm will be given by the following equation:

$$\Delta\text{Abs}_{449} = \varepsilon_{449}^{\text{Cu}} [\text{LCu}^{\text{I}}] + \varepsilon_{449}^{\text{CuO}_2} [\text{LCuO}_2] \quad (4)$$

where ε₄₄₉^{Cu} and ε₄₄₉^{CuO₂} are the extinction coefficients of LCu^I and LCuO₂ at 449 nm. Substituting equation (2) in equation (4) and rearranging gives:

$$[\text{LCuO}_2] = \Delta\text{Abs}_{449} / \Delta\varepsilon_{449} \quad (5)$$

where

$\Delta \text{Abs}_{449} = \text{Abs}_{449}^0 - \text{Abs}_{449}$ is the optical density difference at 449 nm before (Abs_{449}^0) and after (Abs_{449}) adding O_2 to LCu^{I}

and

$\Delta \varepsilon_{449} = \varepsilon_{449}^{\text{CuO}_2} - \varepsilon_{449}^{\text{Cu}}$ is the difference between the extinction coefficients of LCuO_2 and LCu^{I} at 449 nm.

Substitution of equation (5) into equation (3) and rearrangement gives the model used to fit the experimental data from the benchtop titration experiments performed in this work:

$$\Delta \text{Abs}_{449} = (K_{\text{O}_2} [\text{LCu}^{\text{I}}]_0 \Delta \varepsilon_{449} [\text{O}_2]) / (1 + K_{\text{O}_2} [\text{O}_2]) \quad (6)$$

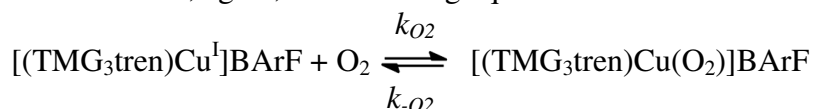
A fit of the experimental points ($[\text{O}_2]$; ΔAbs_{449}) with equation (6) will give the equilibrium constant K_{O_2} (Figure S1).

The same titration measurements performed in a temperature range from -30°C to -70°C give the correspondent values of the equilibrium constants. Data can be fitted with the Van't Hoff equation $\ln(K_{\text{O}_2}) = -(\Delta H^0 / RT) + (\Delta S^0 / R)$ (Figure S2).

6. Model Used for Kinetic Studies

A kinetic "relaxation" method was used as a model for the reaction between $[(\text{TMG}_3\text{tren})\text{Cu}^{\text{I}}]\text{BArF}$ and O_2 where the equilibrium concentrations of the species in solution were perturbed by laser excitation of $[(\text{TMG}_3\text{tren})\text{Cu}(\text{O}_2)]\text{BArF}$ and the return to equilibrium was monitored spectroscopically.

Let's consider, again, the following equilibrium:



Again, $\text{TMG}_3\text{tren} = \text{L}$ and the counter anion BArF was omitted for simplicity. The rate of formation of LCuO_2 will be the following:

$$d[\text{LCuO}_2] / dt = k_{02} [\text{LCu}^{\text{I}}] [\text{O}_2] - k_{-02} [\text{LCuO}_2] \quad (7)$$

At equilibrium, the net rate of formation of LCuO_2 will be zero:

$$d[\text{LCuO}_2] / dt = k_{02} [\text{LCu}^{\text{I}}]_{\text{eq}} [\text{O}_2]_{\text{eq}} - k_{-02} [\text{LCuO}_2]_{\text{eq}} = 0 \quad (8)$$

Upon laser excitation of $[(\text{TMG}_3\text{tren})\text{Cu}(\text{O}_2)]\text{BArF}$ we will alter the concentration of the species in solution as follows:

$$[\text{LCu}^{\text{I}}] = [\text{LCu}^{\text{I}}]_{\text{eq}} + \alpha$$

$$[\text{O}_2] = [\text{O}_2]_{\text{eq}} + \alpha \quad (9)$$

$$[\text{LCuO}_2] = [\text{LCuO}_2]_{\text{eq}} - \alpha$$

Substitution of equations (9) into equation (7) and derivative with respect to α gives the following:

$$-d\alpha / dt = k_{\text{O}_2} [\text{LCu}^{\text{I}}]_{\text{eq}} [\text{O}_2]_{\text{eq}} - k_{-02} [\text{LCuO}_2]_{\text{eq}} + k_{\text{O}_2} \alpha ([\text{LCu}^{\text{I}}]_{\text{eq}} + [\text{LCuO}_2]_{\text{eq}}) + k_{\text{O}_2} \alpha^2 + k_{-02} \alpha$$

The summation of the first two terms on the right side of the equation is zero according to equation (8) and the term " $k_{\text{O}_2} \alpha^2$ " can be neglected since α is small. Consequently, the equation becomes:

$$-d\alpha / dt = \alpha (k_{\text{O}_2} [\text{LCu}^{\text{I}}]_{\text{eq}} + k_{\text{O}_2} [\text{O}_2]_{\text{eq}} + k_{-02})$$

which gives a first order decay of α over time with decay constant:

$$k_{\text{obs}} = k_{\text{O}_2} ([\text{LCu}^{\text{I}}]_{\text{eq}} + [\text{O}_2]_{\text{eq}}) + k_{-02}$$

In our experiments, $[\text{O}_2] \gg [\text{LCu}^{\text{I}}]$ so we can assume that $[\text{LCu}^{\text{I}}]_{\text{eq}} + [\text{O}_2]_{\text{eq}} \approx [\text{O}_2]_0$ where $[\text{O}_2]_0$ is the total concentration of O_2 present in solution at all times. The observed rate constant is then

$$k_{\text{obs}} = k_{\text{O}_2} [\text{O}_2]_0 + k_{-02} (10)$$

Fitting the experimental data ($[\text{O}_2]_0 ; k_{\text{obs}}$) with equation (10) will, then, give a line with slope k_{O_2} and intercept k_{-02} (Figure S3).

The same measurements performed in a temperature range from -40°C to -65°C gave the corresponding rate constants. Data were fitted with the Eyring equation $\ln(k h / k_{\text{B}} T) = - (\Delta H^\ddagger / RT) + (\Delta S^\ddagger / R)$ (where h = Planck constant, k_{B} = Boltzmann constant, T = temperature, and k = rate constant) for both k_{O_2} and k_{-02} . Temperature dependence studies were performed with both 436 nm and 683 nm excitation wavelengths (Figure S4).

Equilibrium constants K_{O_2} were calculated from the ratio k_{O_2} / k_{-02} at each temperature and the relative Van't Hoff plot was determined (Figure S5).

7. Quantum Efficiency Measurements

Samples were prepared by bubbling $\text{O}_{2(\text{g})}$ in solutions of $[(\text{TMG}_3\text{tren})\text{Cu}^{\text{I}}]\text{BArF}$ and $[(\text{PV-TMPA})\text{Cu}^{\text{I}}]\text{BArF}$ in dried and distilled 2-MeTHF at -130°C . The absorbance of the samples at 436 nm and 683 nm (i.e. 0.082 at 683 nm) were monitored using a Cary 50 Bio spectrophotometer equipped with a liquid nitrogen chilled Unisoku USP-203-A cryostat. Two

actinometers were used: $[\text{Ru}(\text{bpy})_3]\text{Cl}_2$ in CH_3CN at room temperature (RT) for the measurement at 436 nm and $[\text{Os}(\text{bpy})_3](\text{PF}_6)_2$ in CH_3CN at RT for the measurements at 683 nm and their solutions were prepared to ensure to match the optical density of $[(\text{TMG}_3\text{tren})\text{Cu}(\text{O}_2)]\text{BArF}$ and $[(\text{PV-TMPA})\text{Cu}(\text{O}_2)]\text{BArF}$ at the relative excitation wavelengths. Data collection for the change in absorbance (ΔA) at the correspondent λ_{max} values (450 nm) where the change in extinction coefficients ($\Delta \epsilon$) are known was made. The quantum yield at the two excitation wavelengths were calculated with equation (11):

$$\Phi(\text{LCuO}_2) = (\Delta A_{450}^{\text{Cu}} / \Delta A_{450}^{\text{Actin}}) (\Delta \epsilon_{450}^{\text{Actin}} / \Delta \epsilon_{450}^{\text{Cu}}) (n_{\text{MeTHF}}^2 / n_{\text{CH}_3\text{CN}}^2) \quad (11)$$

where "Actin" is $[\text{Ru}(\text{bpy})_3]\text{Cl}_2$ in CH_3CN at RT for the 436 nm excitation wavelength and $[\text{Os}(\text{bpy})_3](\text{PF}_6)_2$ in CH_3CN at RT for the 683 nm excitation wavelength. The values $\Delta \epsilon_{450}^{[\text{Ru}(\text{bpy})_3]\text{Cl}_2} = -10600 \text{ M}^{-1} \text{ cm}^{-1}$, $\Delta \epsilon_{450}^{[\text{Os}(\text{bpy})_3](\text{PF}_6)_2} = -7300 \text{ M}^{-1} \text{ cm}^{-1}$, $\Delta \epsilon_{450}^{\text{Cu}} \equiv \Delta \epsilon_{450}^{[(\text{TMG}_3\text{tren})\text{Cu}(\text{O}_2)]\text{BArF}} = -3134 \text{ M}^{-1} \text{ cm}^{-1}$ and $\Delta \epsilon_{450}^{\text{Cu}} \equiv \Delta \epsilon_{450}^{[(\text{PV-TMPA})\text{Cu}(\text{O}_2)]\text{BArF}} = 5531 \text{ M}^{-1} \text{ cm}^{-1}$ (determined in this work) were used. For the refractive index, the value 1.34163 for CH_3CN ($n_{\text{CH}_3\text{CN}}$) at 298.15 K has been used⁹ whereas a temperature correction of 0.00045 per Kelvin has been added to the refractive index of 2-MeTHF at 293.15 K (1.40751)¹⁰ to obtain the refractive index which has been used for 2-MeTHF at 143.15 K in equation (11) (n_{MeTHF}): $1.40751 + [0.00045 \cdot (293.15 - 143.15)] = 1.47501$.

8. DFT Calculations

The calculations were performed with ORCA 2.9.0 program.¹¹ A DFT spin-unrestricted formalism has been used and the Becke88¹² exchange and Perdew86¹² correlation nonlocal functionals were used as implemented in ORCA (BP86) for geometry optimizations whereas the Becke's three-parameter hybrid functional with the correlation functional of Lee, Yang, and Parr (B3LYP)¹³ was used for the single point calculations as well as for the relaxed energy scans done to examine the reaction pathway. The def-2-TZVP basis set¹⁴ present in ORCA was used for all atoms. Relativistic effects were accounted for through the ZORA¹⁵ module implemented in ORCA and also Van der Waals forces¹⁶ were considered in the calculations. Relaxed energy scans along the copper-oxygen distance were performed on the ground state triplet potential energy surface of $[(\text{TMG}_3\text{tren})\text{Cu}(\text{O}_2)]^+$. Results from TD-DFT calculations using localized orbitals are shown in Figure S6 and the DFT calculated O-O bond distance (S7) as a function of the Cu-O distance along the reaction pathway.

9. Table S(1): Comparison of Equilibrium Parameters Determined with Two Different Methods

Table S1. Comparison of Thermodynamic Parameters for O₂ binding to [(TMG₃tren)Cu^I]⁺ determined with two different methods in 2-MeTHF solvent.

Experiment	$\Delta H^{\circ,a}$	$\Delta S^{\circ,b}$
Laser ($\lambda_{exc}=436$ nm)	-35 ± 7	-112 ± 35
Benchtop Titration	-40 ± 2	-134 ± 11
Previous work ⁶	-35 ± 3	-96 ± 13

^a ΔH° values are in kJ mol⁻¹ ^b ΔS° values are in J K⁻¹mol⁻¹

10. Figure S(1): Fit for the Determination of the Equilibrium Constant at -65⁰C

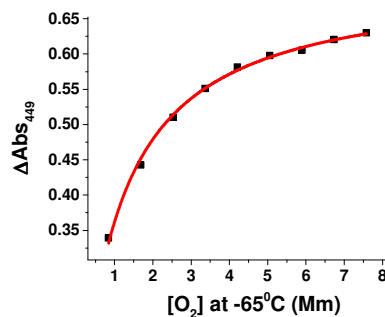


Figure S1. Determination of the equilibrium constant for the binding of [(TMG₃tren)Cu^I]BArF to O₂ at -65⁰C in 2-MeTHF solvent.

11. Figure S(2): Van't Hoff Plot Determined from Benchtop Titration Experiments

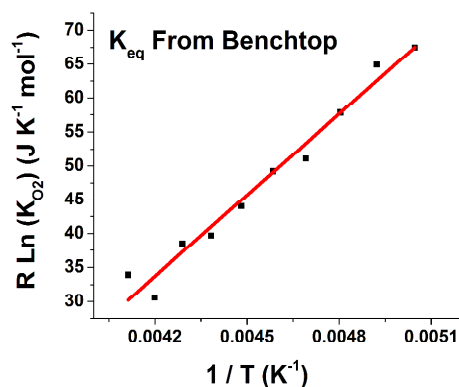


Figure S2. Van't Hoff plot for the variable temperature K_{O_2} data for the binding of $[(TMG_3tren)Cu^I]BARF$ to O_2 in 2-MeTHF solvent.

12. Figure S(3): Determination of k_{O_2} and k_{-O_2} in Pseudo-First-Order Conditions

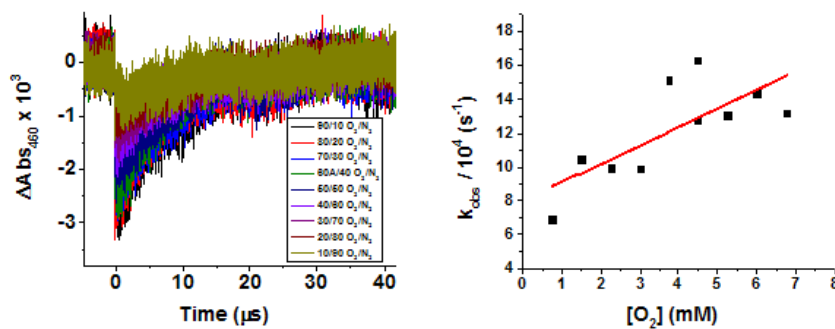


Figure S3. Left: Representative absorption changes monitored at 460 nm at various ratios of $O_{2(g)}/N_{2(g)}$ at $-40^\circ C$ in 2-MeTHF for $[(TMG_3tren)Cu^I]^+ + O_2$. Right: determination of k_{O_2} and k_{-O_2} fitting data with equation (10).

13. Figure S(4): Eyring Analysis on Data Obtained from Transient Absorption Spectroscopy Exciting with either $\lambda_{\text{exc}} = 436$ nm or $\lambda_{\text{exc}} = 683$ nm Light

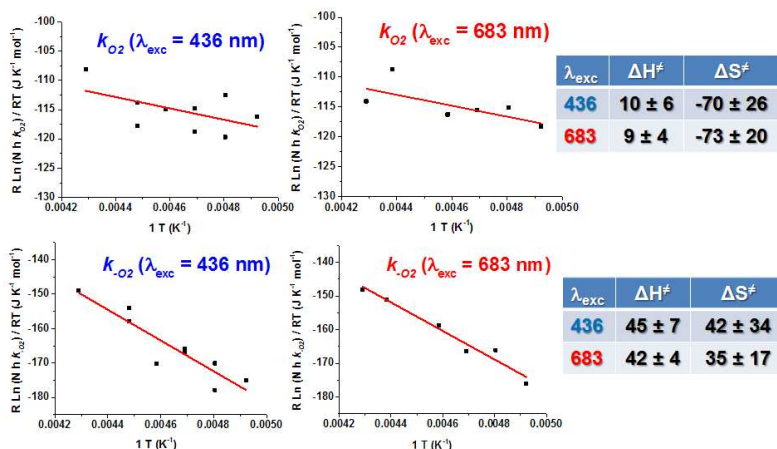


Figure S4. Determination of the activation parameters for the rate constants k_{O_2} and k_{-O_2} for $[(\text{TMG}_3\text{tren})\text{Cu}]^+$ and $[(\text{TMG}_3\text{tren})\text{CuO}_2]^+$.

14. Figure S(5): Van't Hoff Plot Determined from Transient Absorption Spectroscopic Data

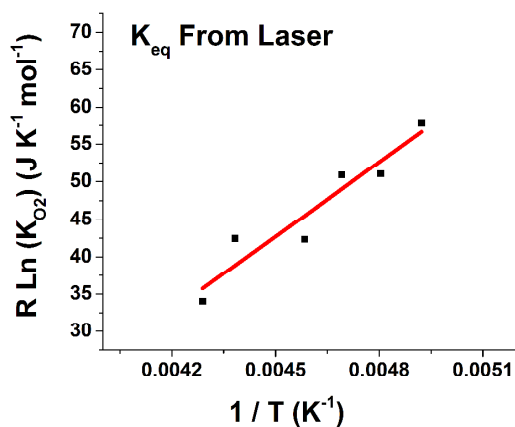


Figure S5. Van't Hoff plot for the equilibrium constants K_{O_2} determined through transient absorption spectroscopy.

15. Figure S(6): Molecular Orbital Diagram for the [(TMG₃tren)Cu(O₂)]⁺ Ground State

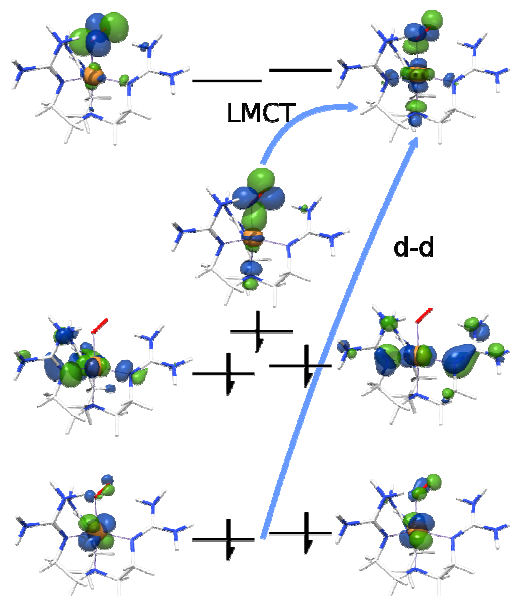


Figure S6. Localized orbital description for [(TMG₃tren)Cu(O₂)]⁺.

16. Figure S(7): Calculated O-O Bond Length Trend upon Cu-O Bond Stretching

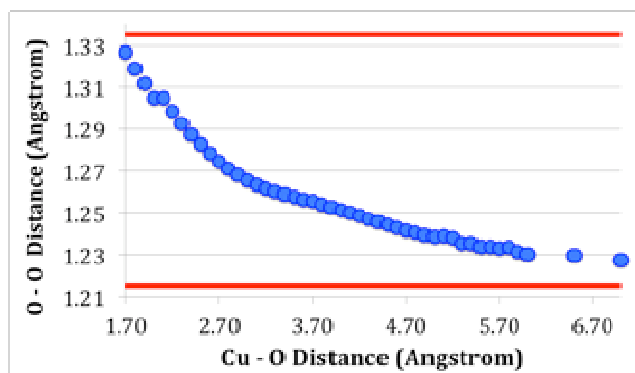


Figure S7. The O-O bond length decreases along the reaction pathway as the Cu-O bond length increases.

17. Figure S(8): Relation Between K_{O_2} and Solvent Dielectric Constant

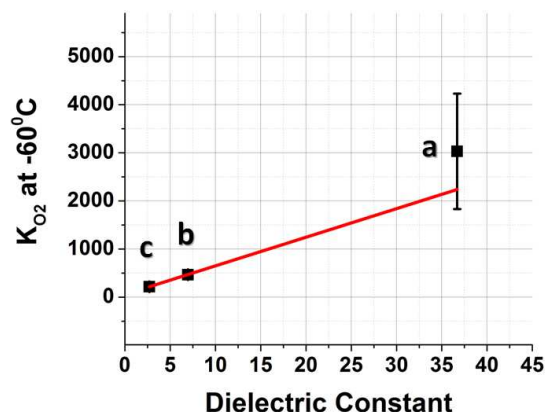


Figure S8. K_{O_2} values determined at -60°C in different solvents as follows: a) $K_{O_2}(\text{DMF}) = 3030 \pm 4340$ from Lanci et al. *J. Am. Chem. Soc.* **2007**, *129*, 14697; b) $K_{O_2}(\text{MeTHF}) = 467 \pm 26$ determined in this work; c) $K_{O_2}(\text{chlorobenzene}) = (K_{O_2}(\text{DMF}) / 14) = 216$ estimated from Lanci et al. *J. Am. Chem. Soc.* **2007**, *129*, 14697 and Lide, D. R. *CRC Handbook of Chemistry and Physics*, 74th ed.; CRC Press: Boca Raton, 1993. Dielectric constants for DMF, MeTHF, and chlorobenzene were taken as 37, 7, and 2.7, respectively

18. Figure S(9): Transient Absorption Spectra Obtained for **1** using $\lambda_{\text{exc}} = 436$ and 683 nm light

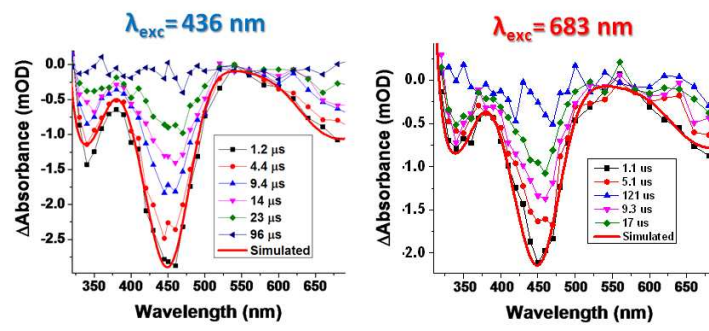


Figure S9. Transient absorption difference spectra collected at the indicated delay times after 436 nm and 683 nm laser excitation of **1** in MeTHF at 218 K. Overlaid in red on the experimental data is a simulated spectrum ($\text{Abs}(\mathbf{3}) - \text{Abs}(\mathbf{1})$)

19. Figure S(10): Absorption Spectra and Transient Absorption Spectra of 2 and 4

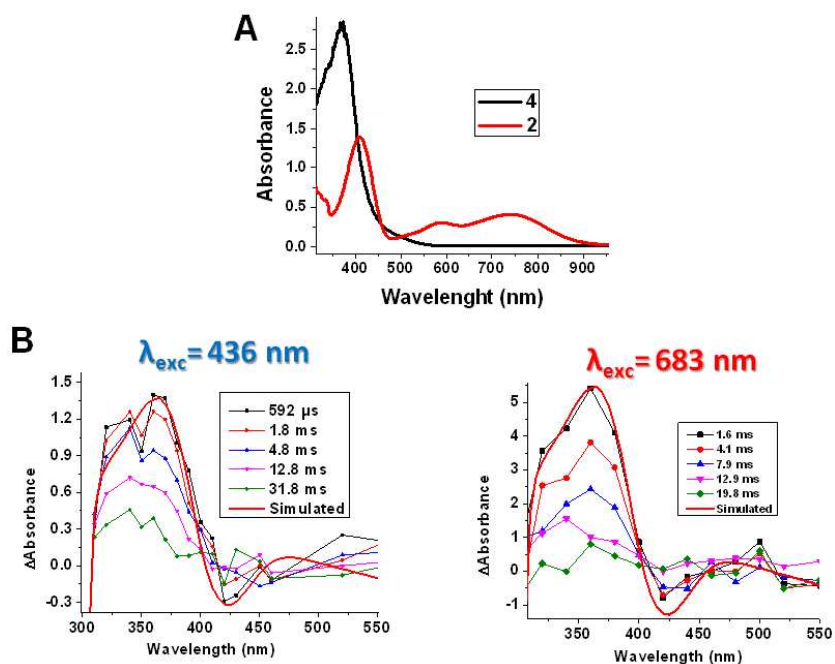


Figure S10. (A) Absorption spectrum of **2** (red line) obtained from oxygenation of **4** (black line) at 143 K in MeTHF. (B) Transient absorption difference spectra collected at the indicated delay times after 436 nm and 683 nm laser excitation of **2** in MeTHF at 143 K. Overlaid in red on the experimental data is a simulated spectrum (Abs(**4**)- Abs(**2**))

20. Figure S(11): Estimation of Activation Parameters for $4 + O_2 \rightarrow 2$: Eyring plot

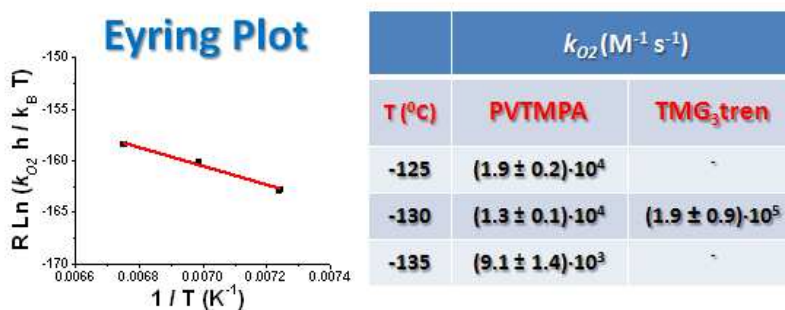


Figure S11. Determination of the activation parameters for the reaction between $[(PVTMPA)Cu]^+$ and O_2 following laser excitation ($\lambda_{exc} = 436$ nm) of $[(PV-TMPA)CuO_2]^+$ in

the temperature range 138 K to 148 K in MeTHF and comparison with the rate constant for the reaction between $[(\text{TMG}_3\text{tren})\text{Cu}^{\text{I}}]^+$ and O_2 extrapolated at 143 K

21. References

- (1) (a) Raab, V.; Kipke, J.; Burghaus, O.; Sundermeyer, J., *Inorg. Chem.* **2001**, *40*, 6964;(b) Liang, H. C.; Kim, E.; Incarvito, C. D.; Rheingold, A. L.; Karlin, K. D., *Inorg. Chem.* **2002**, *41*, 2209.
- (2) Peterson, R. L.; Himes, R. A.; Kotani, H.; Suenobu, T.; Tian, L.; Siegler, M. A.; Solomon, E. I.; Fukuzumi, S.; Karlin, K. D., *J. Am. Chem. Soc.* **2011**, *133*, 1702.
- (3) Fischer, K.; Wilken, M., *J. Chem. Thermodyn.* **2001**, *33*, 1285.
- (4) Battino, R., *IUPAC Solubility Data Series: Oxygen and Ozone; Pergamon: Oxford, New York* **1981**.
- (5) Argazzi, R.; Bignozzi, C. A.; Heimer, T. A.; Castellano, F. N.; Meyer, G. J., *J. Phys. Chem.* **1994**, *33*, 5741.
- (6) Lanci, M. P.; Smirnov, V. V.; Cramer, C. J.; Gauchenova, E. V.; Sundermeyer, J.; Roth, J. P., *J. Am. Chem. Soc.* **2007**, *129*, 14697.
- (7) Yoshimura, A.; Hoffman, M. Z.; Sun, H., *J. Photochem. Photobiol. A* **1993**, *70*, 29.
- (8) Bergeron, B. V.; Kelly, C. A.; Meyer, G. J., *Langmuir* **2003**, *19*, 8389.
- (9) Iloukhani, H.; Almasi, M., *Thermochim. Acta* **2009**, *495*, 139.
- (10) Preus, S.; Kilsa, K.; Wilhelmsson, L. M.; Albinsson, B., *Phys. Chem. Chem. Phys.* **2010**, *12*, 8881.
- (11) Neese, F., *ORCA, version 2.9.0; Max-Planck Institut für Bioanorganische Chemie: Mülheim, Germany*.
- (12) Perdew, J. P., *Phys. Rev. B* **1986**, *33*, 8822.
- (13) (a) Becke, A. D., *Phys. Rev. A* **1988**, *38*, 3098;(b) Becke, A. D., *J. Chem. Phys.* **1993**, *98*, 1372;(c) Becke, A. D., *J. Chem. Phys.* **1993**, *98*, 5648.
- (14) (a) Schaefer, A.; Horn, H.; Ahlrichs, R., *J. Chem. Phys.* **1992**, *97*, 2571;(b) Weigend, F.; Ahlrichs, R., *Phys. Chem. Chem. Phys.* **2005**, *7*, 3297.
- (15) (a) van Lenthe, E.; Baerends, E. J.; Snijders, J. G., *J. Chem. Phys.* **1993**, *99*, 4597;(b) van Wullen, C., *J. Chem. Phys.* **1998**, *109*, 392.
- (16) (a) Grimme, S.; Anthony, J.; Ehrlich, S.; Krieg, H., *J. Chem. Phys.* **2010**, *132*, 154104;(b) Grimme, S., *J. Comput. Chem.* **2006**, *27*, 1787;(c) Grimme, S., *J. Comput. Chem.* **2004**, *25*, 1463.
- (17) Sinnecker, S.; Rajendran, A.; Klamt, A.; Diedenhofen, M.; Neese, F., *J. Phys. Chem. A* **2006**, *110*, 2235.